O^6-Alkylguanine-DNA Alkyltransferase: Low pK_a and High Reactivity of Cysteine 145†

F. Peter Guengerich,*,‡ Qingming Fang,§ Liping Liu,§,|| David L. Hachey,‡ and Anthony E. Pegg§

Department of Biochemistry and Center in Molecular Toxicology, Vanderbilt University School of Medicine, Nashville, Tennessee 37232, and Department of Cellular and Molecular Physiology, The Pennsylvania State University College of Medicine, Hershey, Pennsylvania 17033

Received June 2, 2003; Revised Manuscript Received July 24, 2003

ABSTRACT: The active site cysteine of human O^6-alkylguanine-DNA alkyltransferase (hAGT), Cys145, was shown to be highly reactive with model electrophiles unrelated to substrates, including 1-chloro-2,4-dinitrobenzene. The high reactivity suggested that the Cys145 thiolate anion might be stable at neutral pH. The pK_a was estimated from plots of UV spectra (A_{239}) and reactivity toward 4,4'-dithiopyridine vs pH. The estimated pK_a for hAGT was 4−5, depending upon the method used, and near that of the extensively characterized papain Cys25. Rates of reaction with 4,4'-dithiopyridine were similar for the thiolate forms of hAGT, papain, glutathione, and the bacterial hAGT homologue Ogt (the pK_a of the latter was 5.4). Bound Zn^{2+} has previously been shown to be required for the catalytic activity of hAGT (Rasimas, J. J. et al. (2003) *Biochemistry 42*, 980−990). Zn^{2+} was shown to be required for the low pK_a of hAGT. The high reactivity of hAGT Cys145 is postulated to be important in normal catalytic function, in cross-linking reactions involving bis-electrophiles, and in inhibition of the DNA repair function of hAGT by electrophiles.

The enzymatic repair of chemical damage to DNA is necessary to prevent toxicity and mutation. Many proteins are involved in DNA repair. Some of the most direct repair reactions involve the dealkylation at damaged sites by DNA alkyltransferases. Mammalian AGTs[1] are among the simplest of these and transfer alkyl groups from DNA to a protein Cys group (*1*−*5*).

hAGT has been extensively characterized (*6*−*8*). The protein does not act in a true catalytic sense in that it does not undergo multiple turnovers. However, considerable evidence supports a critical role in protection of human tissues (*7*, *9*). The active site residue is Cys145, which is activated through a charge relay involving His146 and Glu172 (*8*). The X-ray structure also revealed the presence of a bound Zn^{2+} ion (*8*), and biochemical studies have provided evidence for the role of bound Zn^{2+} in catalysis (*10*).

Although AGT has a role in preventing toxicity and mutation by alkylating agents, several reports indicate that AGT can enhance both the toxicity and mutagenicity of 1,2-dibromoethane and dibromomethane in bacterial and mammalian cells (*11*−*16*). A number of possible explanations could be proposed to explain this phenomenon. We have shown that hAGT reacts directly with 1,2-dibromoethane and with 2-bromoethanol, and the reaction with 1,2-dibromoethane leads to cross-linking of AGT to DNA (*17*).

These studies with 1,2-dibromoethane led us to investigate the general reactivity of Cys145 of hAGT, particularly with molecules unrelated to alkylated DNA bases, the traditional substrates. Using a series of spectroscopic and kinetic approaches, we show that the Cys145 in hAGT exists as a reactive thiolate anion at neutral pH. The low pK_a of Cys145 is dependent upon the bound Zn^{2+}, explaining the previous observations on its role (*10*).

EXPERIMENTAL PROCEDURES

Reagents. CDNB (Aldrich Chemical Co., Milwaukee, WI) was recrystallized from C_2H_5OH. 4-Aldrithiol (4,4'-dithiopyridine) was purchased from Aldrich and used without further purification.

Proteins and Enzymes. hAGT and the mutant hAGT C145S (with C-terminal $(His)_6$ tags) were expressed in *Escherichia coli* and purified as described (*10*, *18*, *19*). Zn^{2+}-depleted and Zn^{2+}-enriched samples of hAGT were prepared as described and contained <0.1 and 2.9 g-atoms Zn^{2+} (mol hAGT)$^{-1}$, respectively, as judged by inductively coupled plasma-mass spectrometry (*10*). hAGT concentrations were estimated using $\epsilon_{280} = 3.93 \times 10^4$ M^{-1} cm^{-1} (*10*, *20*).

E. coli Ada-C and Ogt were prepared from overexpression systems using plasmids pQE30-Ada-C and pQE30-Ogt (in *E. coli*) and purified using the described methods (*21*).

† Supported by U.S. Public Health Service Grants R01 ES10546 (F.P.G.), P30 ES00267 (F.P.G.), R01 CA18137 (A.E.P.), and R01 CA97209 (A.E.P.).

* Corresponding author. Tel: (615) 322-2261. Fax: (615) 322-3141. E-mail: f.guengerich@vanderbilt.edu.

‡ Vanderbilt University.

§ Pennsylvania State University.

|| Present address: Abramson Family Cancer Institute, University of Pennsylvania, 421 Curie Blvd., 438 BRB II/III, Philadelphia, PA 19104.

[1] Abbreviations used: (h)AGT, (human) O^6-alkylguanine-DNA alkyltransferase; CDNB, 1-chloro-2,4-dinitrobenzene; GSH, glutathione; HPLC/MS, high performance liquid chromatography/mass spectrometry.

10.1021/bi034937z CCC: $25.00
Published on Web 08/29/2003

Papain (from *Papaya latex*) was purchased from Sigma Chemical Co. (St. Louis, Mo) and activated by treatment with 5 mM tris-(carboxyethyl)phosphine (*22*) overnight (4 °C) (quantified using $E_{278}^{1\%} = 25.0$ cm^{-1} (*23*)).

Prior to obtaining spectra of proteins or use in reactions, reductant (dithiothreitol or tris-(carboxyethyl)phosphine (*22*)) was removed by 3−4 dialyses (100-fold volume each time) over 24−40 h (at 4 °C) vs 20 mM Tris·HCl buffer (pH 8.0) containing 0.50 M NaCl (and 0.1 mM EDTA except in the case of Zn^{2+}-depleted and -enriched hAGT), thoroughly purged with N_2 gas (in sealed Erlenmeyer flasks).

CDNB Reactions. hAGT (6 μM) was added to a cuvette (volume 1.0 mL) containing 0.10 M potassium *N*-(2-hydroxyethylpiperazine)-*N*'-(2-ethanesulfonate) and allowed to equilibrate at 37 °C for 3 min in a Cary14/OLIS spectrophotometer (OLIS, Bogart, GA). A 10-μL aliquot of each stock solution of CDNB (in C_2H_5OH) was added, and the change in A_{360} was monitored as a function of time for 5 min. The portion of the resulting trace that showed first-order kinetics (log A_{360} vs time) was used to calculate the rate.

In a separate experiment, hAGT (1.5 nmol in 0.15 mL of the same buffer) was racted with a substoichiometric amount of CDNB (1.0 nmol) for 8 min, and preliminary HPLC/MS (electrospray) analysis indicated that modification had occurred. The sample was digested with bovine trypsin (Worthington, Freehold, NJ, TCPK grade, 1:10 ratio of trypsin to hAGT, w/w) for 2 h at 37 °C in 0.10 M $NaHCO_3$ buffer (pH 8.0) (*17*). An aliquot was analyzed by HPLC/MS under conditions similar to those described previously (*17*), except that an LCQ instrument (Finnigan-MAT, San Jose, CA) was used, in the positive ion electrospray mode.

UV Spectral Titrations. Following dialysis to remove reductants (vide supra), aliquots of hAGT, Ada-C, or Ogt (0.10 mL) were diluted with 0.40 mL of 0.25 M potassium phosphate of varying pH, and UV spectra were recorded at 23 °C in a Cary14/OLIS spectrophotometer (330 to 230 nm, 10 mm path length, three spectra averaged in the instrument except at pH < 5, at which some samples were less stable and only a single spectrum was recorded). The ratio A_{239}/A_{280} was used with the known ϵ_{280} of hAGT (3.93×10^4 M^{-1} cm^{-1}) (*10*, *20*) to calculate ϵ_{239}, which was plotted vs pH.

Data points were fit with Graphpad Prism (Graphpad, San Diego, CA) using nonlinear regression fitting to the equation $Y = [(Y_{min}\,10^{-X}) + (Y_{max}\,10^{-pKa})]/(10^{-X} + 10^{-pKa})$ (*24*), with SE calculated by the software program and indicated as "± ".

Rates of Reaction with 4,4′-Dithiopyridine. Either hAGT or the hAGT C145S mutant (1.9−12.5 μM), Ogt (12 μM), papain (100 μM), or GSH (100 μM) in 20 mM Tris·HCl, pH 8.0 (under N_2) was transferred to one syringe of an OLIS RSM-1000 stopped-flow spectrophotometer (OLIS, Bogart, GA). The other syringe contained 100 μM 4,4′-dithiopyridine (200 μM in cases of papain and GSH) dissolved in 0.20 M potassium phosphate buffer of the desired pH. Aliquots from each syringe were mixed, and the change in A_{324} was monitored in the fixed-wavelength mode (24 °C). Data were fit to biphasic plots (monoplasic with slower low pH reactions). The rates of the fast-phase reactions were measured using the OLIS software and plotted vs pH, fitting to the same equation as presented under UV Spectral Titrations (vide supra). Most rates are presented as means of two or three determinations (from subsequent reactions); in some cases traces from individual reactions were averaged in the instrument before estimation of rates.

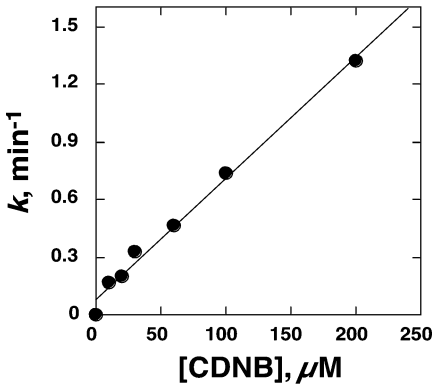

FIGURE 1: Rate of reaction of AGT with CDNB. Varying concentrations of CDNB were added to AGT (6 μM) and the apparent first-order rates of reaction were estimated from plots of A_{360} vs time. These rates were plotted vs the CDNB concentration; linear correlation analysis yielded a second-order rate constant of 1.4×10^3 M^{-1} s^{-1}.

RESULTS

Reaction of hAGT with CDNB. CDNB is an electrophile that reacts with activated thiols (*25*). Previous studies have indicated that the thiolate anionic is much more reactive than the (protonated) thiol (*26*). The reaction can be monitored by the increase in A_{360} (*25*).

hAGT was reacted with a substoichiometric amount of CDNB (0.67 mol equiv). HPLC analysis of the tryptic digest indicated the presence of a major modified peptide (A_{360} measurements). HPLC/MS analysis of this peptide by collision-induced dissociation confirmed its identity as the 136−147 peptide with Cys145 as the site of attachment of the 2,4-dintrophenyl (see Supporting Information for fragmentation spectrum and *b* and *y* ion assignments). A small amount of modification of peptide 148−165 (Cys150) was also noted.

hAGT was reacted with CDNB at pH 7.6. Rates of the pseudo- first-order reaction of CDNB with hAGT were measured and plotted vs the CDNB concentration to yield a second-order rate constant of 1.4×10^3 M^{-1} s^{-1} (Figure 1).

UV Spectral Titration of Cys145 of hAGT. The high reactivity of hAGT with CDNB (vide supra) suggested that a thiolate anion (of Cys145) might exist at neutral pH and react, because thiolates (RS^-) are several orders of magnitude more reactive than the respective protonated thiols (RSH) (*27*−*29*). Thiolate anions can be distinguished from protonated thiols by increased absorbance at 235−240 nm (*30*).

Preliminary analysis of hAGT, devoid of exogenous stabilizing thiols, showed a pH-dependent change in absorbance (see Supporting Information for difference spectra). Analysis of the spectra as a function of pH yielded a sigmoidal plot with a pK_a of 6.7 (Figure 2). The change was not seen in the hAGT C145S mutant (until pH 9.1, when other thiols are also titrated). The $\Delta\epsilon_{239}$ was $\sim 4.5 \times 10^3$ M^{-1} cm^{-1}, similar to that reported for other thiolates, (e.g. GSH $\rightleftharpoons$ GS^- + H^+, 5.2×10^3 M^{-1} cm^{-1})(*30*).

Reaction of hAGT and Other Thiols with 4,4′-Dithiopyridine. Protein thiols can be titrated with disulfide reagents

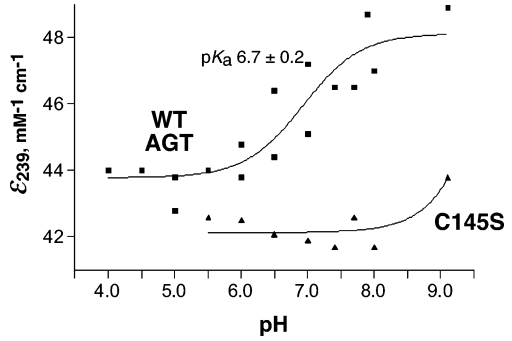

FIGURE 2: pH titration of AGT (■) and AGT C145S (▲) monitored by UV spectra. UV spectra were measured as described under Experimental Procedures (see also Supporting Information). A_{239} was plotted vs pH to yield a pK_a value of 6.7 ± 0.2 for AGT. The program yielded an estimate of 8.2 for AGT C145S, but this value is probably an underestimate, as suggested in the subsequent figures.

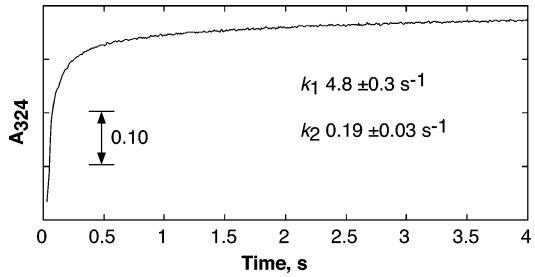

FIGURE 3: Reaction of AGT with 4,4'-dithiopyridine. AGT (12.5 μM in 0.20 M potassium phosphate buffer, pH 8.0, under an N_2 atmosphere) was mixed with 200 μM 4,4'-dithiopyridine in the stopped-flow instrument, and the change in A_{324} was recorded vs time and fit to a biphasic plot using the OLIS software: $k_1 = 4.8 \pm 0.3$ s^{-1}, $k_2 = 0.19 \pm 0.03$ s^{-1}.

that generate chromophores upon reaction (i.e. release of thiol or thiolate chromophore). 4,4′-Dithiopyridine was selected for use from preliminary trials with that reagent, 2,2′-dithiopyridine, and 5,5′-dithio-bis(2-nitrobenzoic acid) (Ellman's reagent) (*31*). Reaction of 4,4′-dithiopyridine with hAGT yielded a biphasic plot at pH 8.0 (Figure 3), with the change in A_{324} in the fast phase corresponding to reaction with a single sulfhydryl. The first reaction was not observed in the hAGT C145S mutant.

Rates of reaction of hAGT with 4,4′-dithiopyridine were measured at different pH values (Figure 4). The fast phase could be plotted vs pH to yield an apparent pK_a of 5.3. The rate of the slow phase of the reaction did not increase until >pH 9 and was insignificant compared to the fast phase. For comparison, the reaction with GSH yielded a pK_a of 8.9 (Figure 4). The well-characterized cysteine protease papain, with the reactive Cys25, yielded a pK_a of 4.6, similar to the value of 4.1 reported by Shaked et al. (*29*). The maximum pseudo-first-order rates measured with hAGT and papain were similar (~3.5 s^{-1}) and only slightly less than those measured for GSH (maximum ≈ 5 s^{-1}).

Estimates of pK_a Values of Bacterial Alkyltransferases. Bacterial homologues of hAGT were studied to determine if they also showed low pK_a values. *E. coli* has two O^6-alkylguanine-DNA alkyl transferases, the constitutive Ogt and the inducible Ada (*32*, *33*). The Ada protein has two active sites, one of which is located in the C-terminal domain and carries out repair of O^6-methylguanine in DNA. The Ada-C protein representing this domain has been widely studied as an AGT, and its crystal structure is known (*34*).

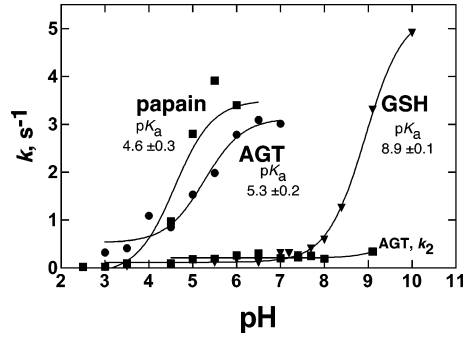

FIGURE 4: Reactivity of AGT (●), papain (■), and GSH (▼) with 4,4′-dithiopyridine as a function of pH. Apparent first-order rates of reaction were estimated using stopped-flow spectrophotometric measurements as described under Experimental Procedures and Figure 3. The slower rate (k_2) from the AGT reaction (Figure 3) was also plotted. The estimates of pK_a were: AGT, 5.3 ± 0.2; papain, 4.6 ± 0.3; GSH, 8.9 ± 0.1.

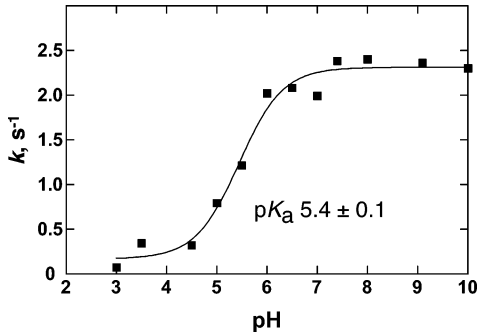

FIGURE 5: Reactivity of *E. coli* Ogt with 4,4′-dithiopyridine as a function of pH. The measurements were made as for Figures 3 and 4. The estimated pK_a value was 5.4 ± 0.1.

Efforts to measure pK_a values from UV spectra (ϵ_{239}) were difficult because of the turbidity that developed rapidly at pH values <7. The titration of Ada suggested a pK_a of ~5.1 (results not shown), but this value is compromised by the limited spectral data at low pH values. Efforts to record spectra of Ogt at low pH values were completely unsuccessful. However, the rapid reaction of the protein thiols with 4,4'-dithiopyridine permitted the measurement of rates prior to development of turbidity (<1 s time, Figure 3). Ogt yielded a pK_a of 5.4 (Figure 5). The maximum rate for the Ogt reaction was only slightly less (~2.5 s^{-1}) than for hAGT.

Effect of Zn^{2+} on pK_a of hAGT. Other work indicates that the catalytic activity of hAGT is dependent upon the presence of Zn^{2+} (*10*), but the reason for this effect was not elucidated. The experiments with hAGT presented thus far (Figures 1−4) were done with hAGT that had been isolated without attention to changing the presence of Zn^{2+} in the protein, which is generally found at a slightly less than stoichiometric amount (*10*).

The amount of Zn^{2+}/hAGT was adjusted to either <0.1 (Zn^{+}-depleted) or 2.9 (Zn^{2+}-enriched) atoms/molecule by a denaturation/renaturation procedure (*10*). Plotting the UV spectra (ϵ_{239}) vs pH yielded a pK_a of 4.3 for Zn^{2+}-enriched hAGT, but a spectral change was not seen for the Zn^{2+}-depleted protein (Figure 6). A plot of the rates of reaction with 4,4′-dithiopyridine vs pH yielded a pK_a of 3.8 for Zn^{2+}-enriched hAGT (Figure 7). The rate did not increase with Zn^{2+}-depleted hAGT until high pH (pK_a ≈ 8.7) (Figure 7).

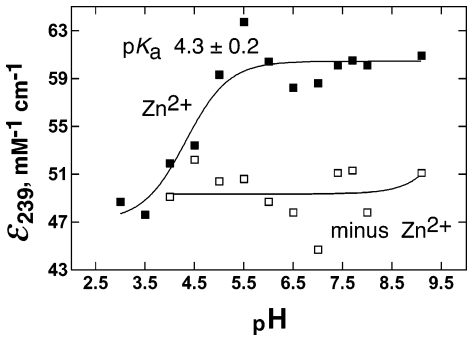

FIGURE 6: pH titrations of Zn^{2+}-fortified (■) and Zn^{2+}-depleted (□) AGT monitored by UV spectrophotometric measurements. The estimated pK_a value was 4.3 ± 0.2 for Zn^{2+}-fortified AGT.

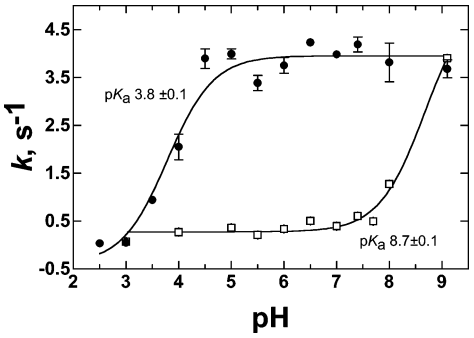

FIGURE 7: Reactivities of Zn^{2+}-fortified (●) and Zn^{2+}-depleted (□) AGT with 4,4'-dithiopyridine as a function of pH. Rates were estimated as described (Figures 3, 4, 6). In the case of Zn^{2+}-fortified AGT, three individual rates were collected, and the results are shown as the mean ± SD. With Zn^{2+}-depleted AGT, the results of three individual reactions were averaged in the OLIS software, and the averaged values were used. The estimated pK_a values were: Zn^{2+}-fortified AGT, 3.8 ± 0.1; Zn^{2+}-depleted AGT, 8.7 ± 0.1.

DISCUSSION

The DNA repair protein hAGT was shown to have a highly reactive Cys in the active site, Cys145. This residue is highly reactive not only with the normal O^6-alkylguanine substrates, DNA-bound and free bases, but also with other electrophiles such as 1,2-dibromoethane, as shown recently in work from our laboratories (*17*). We report here that this high reactivity is related to a low pK_a, as shown by the pH dependence of both the UV spectra and rates of reaction with 4,4'-dithiopyridine. The low pK_a of hAGT is related to the presence of Zn^{2+} in the enzyme, a relationship which can explain the previously reported requirement of Zn^{2+} for catalytic activity (*10*).

The reactivity of Cys145 of hAGT was shown previously in the reactions with 1,2-dibromoethane and 2-bromoethanol, where the Cys145-modified tryptic peptides were identified by mass spectrometry (*17*). The general reactivity of this Cys residue was shown here in the reaction of hAGT with the electrophile CDNB (Figure 1). The estimated second-order rate of the reaction was within a factor of 3 of a previously reported rate measured with GSH thiolate (pH 11) (*26*). The high reactivity of hAGT suggested that the thiolate anion of Cys145 might exist at neutral pH and might explain the reactivity of hAGT.

A low pK_a value of hAGT was initially established using UV spectral measurements (Figure 2), in a procedure used earlier to estimate the pK_a of GSH bound to GSH transferase (*30*). The estimated $\Delta\epsilon_{239}$ (4.5×10^3 M^{-1} cm^{-1}) and control experiments with hAGT C145S provide support that the changes are due to the protonation state of Cys145 (Figure 2). More accurate estimates of pK_a were obtained using the pH dependence of the pseudo-first-order rates of reaction with 4,4'-dithiopyridine (Figure 4). Shaked et al. (*29*) have discussed the advantages of using rates of disulfide exchange to estimate pK_a values of proteins compared to other reactions. This kinetic approach yielded a pK_a (5.3) somewhat lower than the first estimates derived from the UV spectra (Figure 2). The pK_a of the Cys145 of hAGT is ~4 units less than that of GSH (Figure 4). The pK_a values of papain (4.6, cf. 4.1 for Shaked et al. (*29*)) and hAGT (5.3 in this experiment) are similar and suggest that the reactivity of Cys145 of hAGT may be comparable to that of the well-characterized Cys25-thiolate anion of papain. The rates of reactions were relatively similar for hAGT, papain, the bacterial transferase Ogt, and the GSH thiolate (Figures 4, 5). However, the point should be made that factors other than pK_a can also modulate the nucleophilicity of a thiolate anion (*28*, *29*).

Crystal structures are now available for three AGTs (*E. coli* Ada-C, human, and *Pyrococcus kodakaraensis*) (*8*, *34*−*36*). These structural studies have indicated that the protein contains two domains. The role of the N-terminal domain, which is represented by residues 1−85 in hAGT, is unclear but it is essential for AGT stability and for the correct orientation of the carboxyl terminal domain. The C-terminal domain of the AGT contains the active site binding pocket and the DNA binding domain, which is a winged helix−turn−helix motif. The cysteine acceptor site of AGTs is buried in the protein, and in order for reaction with a DNA substrate to take place, the substrate O^6-alkylguanine must be displaced from the DNA helix (*37*). Such displacement places the substrate close to the cysteine acceptor site. The crystal structures indicate that this cysteine is part of a network of amino acids and a bound water linking it to His146, Arg147, and Glu172 (*8*, *34*−*36*). This network may facilitate proton abstraction to the low pK_a of Cys145. The residues forming this network are conserved in all AGTs.

Previous crystallography work has demonstrated the presence of Zn^{2+} in hAGT (*8*), and the importance of bound Zn^{2+} for catalytic activity has been documented (*10*). The effect appears not to be due to any gross effects on protein structure (as judged by fluorescence, CD, and comparison of crystal structures (*8*, *10*, *37*)) or DNA affinity (*10*). The effect is seen in catalytic activity toward the non-DNA substrate O^6-benzylguanine and therefore relates to alkyl group transfer rather than DNA binding (*10*). We found a strong effect of bound Zn^{2+} on the pK_a of hAGT, as judged by the pH dependence of UV spectra and rates of reaction with 4,4'-dithiopyridine (Figures 6, 7). The pK_a of the Zn^{2+}-enriched sample (3.8) was lower than that of any of the previous hAGT preparations examined. The preparation used in our studies that was saturated with Zn^{2+} had three molecules of the metal per molecule of hAGT. The critical Zn^{2+} atom is probably that one which is bound at an internal site within a coordination sphere of four amino acid residues (Cys5, Cys24, His29, and His85) near the N terminus of the protein (*8*). The presence of this Zn^{2+} stimulates catalytic activity 60-fold (*10*). One of the other two Zn^{2+} atoms is very loosely bound to the protein surface and possibly to Cys150, which is in the active site, and is weakly inhibitory

to AGT activity. The presence of Zn^{2+} in the assay buffer inhibits catalytic activity (the effect was not tested in the pK_a determinations), and this effect was blocked by mutation of Cys150 (*10*). The third Zn^{2+} is bound to the polyhistidine tag used for purification and has no effect on catalytic activity (*10*). The internal Zn^{2+} atom is likely to play a key structural role in maintaining the structure of the N-terminal domain and hence the interaction between the two domains of the protein. This in turn may be needed to maintain the interactions between the amino acids at the active site described above. The crystal structures with and without Zn^{2+} are identical in the active site region (*8*, *37*), but the resolution is not sufficient to be certain that there is not a small change which could have a profound effect on the network involving Cys145. This role of Zn^{2+} is quite different from that which has been established for the metal in activating methylphosphotriester repair by the N-terminal domain of the *E. coli* Ada protein (N-Ada) (*33*, *38*, *39*). In this case, the reactive cysteine (Cys69) is actually one of the ligands of the bound Zn^{2+} in N-Ada and directly activates alkyl transfer.

The high reactivity of Cys145 raises some important issues for hAGT (and other low pK_a DNA alkyltransferases). In principle, the protein could be a target for reactive electrophiles. It might be expected to appear in proteomics/toxicogenomics screens (*40*), although this is a relatively low-abundance protein and might not be prominent. Another issue we have already raised is the ability to react with bis-electrophiles and generate cross-linking events (*17*). It is also likely to contribute to the inhibition of hAGT by O^6-benzylguanine (*41*, *42*) although in this case the ability of the substrate analogue to bind and react in the active site pocket via interaction with residues that normally recognize O^6-methylguanine also plays a role.

An important final point is that the function of hAGT in repairing DNA might appear to be highly susceptible to electrophiles that could inactivate hAGT and inhibit the repair of DNA. Direct inactivation of hAGT and Ada-C has been reported to occur after exposure to alkylating agents including methyl methanesulfonate, dimethyl sulfate, methyl iodide, *N*-methyl-*N*-nitrosurea, *N*-methyl-*N*′-nitro-*N*-nitrosoguanidine, streptozotocin, and triazines (*43*−*48*). Direct inactivation by S_N2-reactive agents, which form very little O^6-methylguanine in their reaction with DNA, may account for the loss of AGT in cells treated with these agents (*46*, *48*) and could increase susceptibility to other environmental agents that do form O^6-methylguanine. Similarly, AGT has been shown to be inactivated by aldehydes including acrolein, 4-hydroxyypentenal, 4-hydroxyoctenal, 4-hydroxynonenal, and (more weakly) formaldehyde (*49*, *50*) and this could contribute to the co-carcinogenic potential of such agents, which occur environmentally and as a result of lipid peroxidation. Also, the facile inactivation of hAGT by NO•, which is formed in pathogenic amounts in inflammation and infection, occurs because of the sensitivity of the Cys145 to nitrosylation (*51*, *52*). In all of these cases, the high reactivity of Cys145 may contribute to loss of alkyltransferase-mediated repair capacity and therefore may enhance genotoxicity.

SUPPORTING INFORMATION AVAILABLE

Collision-induced dissociation mass spectrum of peptide 136−147 isolated from CDNB-modified hAGT; pH-dependent UV difference spectra of hAGT. This material is available free of charge via the Internet at http://pubs.acs.org.

REFERENCES

1. Mitra, S., and Kaina, B. (1993) *Prog. Nucleic Acid Res. Mol. Biol. 44*, 109−142.
2. Pegg, A. E., Dolan, M. E., and Moschel, R. C. (1995) *Prog. Nucleic Acid Res. Mol. Biol. 51*, 167−223.
3. Pieper, R. O. (1997) *Pharmacol. Therapeut. 74*, 285−297.
4. Sekiguchi, M., Nakabeppu, Y., Sakumi, K., and Tuzuki, T. (1996) *J. Cancer Res. Clin. Oncol. 122*, 199−206.
5. Margison, G., Povey, A. C., Kaina, B., and Santibáñez-Koref, M. F. (2003) *Carcinogenesis 24*, 625−635.
6. Hazra, T. K., Roy, R., Biswas, T., Grabowski, D. T., Pegg, A. E., and Mitra, S. (1997) *Biochemistry 36*, 5769−5776.
7. Pegg, A. E. (2000) *Mutat. Res. 462*, 83−100.
8. Daniels, D. S., Mol, C. D., Arvai, A. S., Kanugula, S., Pegg, A. E., and Tainer, J. A. (2000) *EMBO J. 19*, 1719−1730.
9. Margison, G. P., and Santibáñez-Koref, M. F. (2002) *BioEssays 24*, 255−266.
10. Rasimas, J. J., Kanugula, S., Dalessio, P. M., Ropson, I. J., Fried, M. G., and Pegg, A. E. (2003) *Biochemistry 42*, 980−990.
11. Foster, P. L., Wilkinson, W. G., Miller, J. K., Sullivan, A. D., and Barnes, W. M. (1988) *Mutat. Res. 194*, 171−181.
12. Abril, N., Ferrezuelo, F., Prieto-Alamo, M. J., Rafferty, J. A., Margison, G. P., and Pueyo, C. (1996) *Carcinogenesis 17*, 1609−1614.
13. Abril, N., Luque-Romero, F. L., Prieto-Alamo, M.-J., Rafferty, J. A., Margison, G. P., and Pueyo, C. (1997) *Carcinogenesis 18*, 1883−1888.
14. Abril, N., and Margison, G. P. (1999) *Chem. Res. Toxicol. 12*, 544−551.
15. Abril, N., Luque-Romero, F. L., Christians, F. C., Encell, L. P., Loeb, L. A., and Pueyo, C. (1999) *Carcinogenesis 20*, 2089−2094.
16. Liu, H., Xu-Welliver, M., and Pegg, A. E. (2000) *Mutat. Res. 452*, 1−10.
17. Liu, L., Pegg, A. E., Williams, K. M., and Guengerich, F. P. (2002) *J. Biol. Chem. 277*, 37920−37928.
18. Edara, S., Kanugula, S., Goodtzova, K., and Pegg, A. E. (1996) *Cancer Res. 56*, 5571−5575.
19. Liu, L., Xu-Welliver, M., and Pegg, A. E. (2001) *FASEB J. 15*, Abstract 519.
20. Roy, R., Shiota, S., Kennel, S. J., Raha, R., von Wronski, M., Brent, T. P., and Mitra, S. (1995) *Carcinogenesis 16*, 405−411.
21. Goodtzova, K., Kanugula, S., Edara, S., Pauly, G. T., Moschel, R. C., and Pegg, A. E. (1997) *J. Biol. Chem. 272*, 8332−8339.
22. Getz, E. B., Xiao, M., Chakrabarty, T., Cooke, R., and Selvin, P. R. (1999) *Anal. Biochem. 273*, 73−80.
23. Worthington, V. (1993) in *Worthington Enzyme Manual*, pp 280−285, Worthington Biochemical Corp., Freehold, NJ.
24. Zhao, G., and Jorns, M. S. (2002) *Biochemistry 41*, 9747−9750.
25. Habig, W. H., Pabst, M. J., and Jakoby, W. B. (1974) *J. Biol. Chem. 249*, 7130−7139.
26. Gan, L.-H. (1977) *Aust. J. Chem. 30*, 1475−1479.
27. Roberts, J. D., and Caserio, M. C. (1965) *Basic Principles of Organic Chemistry*, p 751, W. A. Benjamin, New York.
28. Smith, M. B., and March, J. (2001) *March's Advanced Organic Chemistry: Reactions, Mechanisms, and Structure*, p 496, Wiley-Interscience, New York.
29. Shaked, Z., Szajewski, R. P., and Whitesides, G. M. (1980) *Biochemistry 19*, 4156−4166.
30. Graminski, G. F., Kubo, Y., and Armstrong, R. N. (1989) *Biochemistry 28*, 3562−3568.
31. Egwim, I. O. C., and Gruber, H. J. (2001) *Anal. Biochem. 288*, 188−194.
32. Lindahl, T., Sedgwick, B., Sekiguchi, M., and Nakabeppu, Y. (1988) *Annu. Rev. Biochem. 57*, 133−157.
33. Myers, L. C., Terranova, M. P., Ferentz, A. E., Wagner, G., and Verdine, G. L. (1993) *Science 261*, 1164−1167.
34. Moore, M. H., Gulbus, J. M., Dodson, E. J., Demple, B., and Moody, P. C. E. (1994) *EMBO J. 13*, 1495−1501.
35. Hashimoto, H., Inoue, T., Nishioka, M., Fujiwara, S., Takagi, M., Imanaka, T., and Kai, Y. (1999) *J. Mol. Biol. 292*, 707−716.
36. Wibley, J. E. A., Pegg, A. E., and Moody, P. C. E. (2000) *Nucleic Acid Res. 28*, 393−401.

37. Daniels, D. S., and Tainer, J. A. (2000) *Mutat. Res. DNA Repair 460*, 151−163.
38. Myers, L. C., Verdine, G. L., and Wagner, G. (1993) *Biochemistry 32*, 14089−14094.
39. Sun, L. J., Yim, C. K., and Verdine, G. L. (2001) *Biochemistry 40*, 11596−11603.
40. Qiu, Y., Benet, L. Z., and Burlingame, A. L. (1998) *J. Biol. Chem. 273*, 17940−17953.
41. Dolan, M. E., Moschel, R. C., and Pegg, A. E. (1990) *Proc. Natl. Acad. Sci. U.S.A. 87*, 5368−5372.
42. Pegg, A. E., Boosalis, M., Samson, L., Moschel, R. C., Byers, T. L., Swenn, K., and Dolan, M. E. (1993) *Biochemistry 32*, 11998−12006.
43. Brent, T. P. (1986) *Cancer Res. 46*, 2320−2323.
44. Takahashi, K., Kawazoe, Y., Sakumi, K., Nakabeppu, Y., and Sekiguchi, M. (1988) *J. Biol. Chem. 263*, 13490−13492.
45. Link, A., and Templ, K. (1991) *J. Cancer Res. Clin. Oncol. 117*, 549−545.
46. Sledziewska-Gójska, E. (1995) *Mutat. Res. 336*, 61−67.
47. Lacal, P. M., D'Atri, S., Orlando, L., Bonmassar, E., and Graziani, G. (1996) *J. Pharmacol. Exp. Ther. 279*, 416−422.
48. Oh, H. K., Teo, A. K. C., Ali, R. B., Lim, A., Ayi, T. C., Yarosh, D. B., and Li, B. F. L. (1996) *Biochemistry 35*, 12259−12266.
49. Krokan, H., Grafstrom, R. C., Sundqvist, K., Esterbauer, H., and Harris, C. C. (1985) *Carcinogenesis 6*, 1755−1759.
50. Grafstrom, R. C., Pegg, A. E., Harris, C. C., Sundqvist, K., and Krokan, H. (1986) in *Repair of DNA Lesions Introduced by N-Nitroso Compounds* (Myrnes, B., and Krokan, H., Eds.) pp 154−175, Norwegian University Press, Oslo.
51. Laval, F., and Wink, D. A. (1994) *Carcinogenesis 15*, 443−447.
52. Liu, L., Xu-Welliver, M., Kanugula, S., and Pegg, A. E. (2002) *Cancer Res. 62*, 3037−3043.

BI034937Z